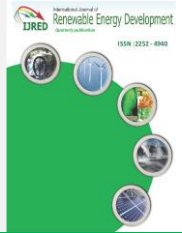




Contents list available at IJRED website

International Journal of Renewable Energy Development

Journal homepage: <https://ijred.undip.ac.id>



Research Article

Design and Optimization of a Rack and Pinion Type WEC Using an Auxiliary Vibrating System

Avikash Kaushik Chand¹, Farid Mahboubi Nasrekani*¹, Kabir Mamun¹, Sumesh Narayan¹

School of Information Technology, Engineering, Mathematics and Physics (STEMP), The University of the South Pacific, Suva, Fiji

Abstract. Research on wave energy converters with Rack and pinion type Power Take-Off (PTO) has been increasing over the last few years. A few control methods are used to optimize the performance of the said Wave Energy Converters (WECs). This paper presents a novel auxiliary vibrating system that can be implemented to improve the power input to a wave energy converter with a rack and pinion type PTO in regular waves. The design of the WEC system includes a floater, a double rack and pinion arrangement, a vibrating system, and a Mechanical Motion Rectifier (MMR) consisting of two one-way bearings that can convert the bidirectional wave motion to a unidirectional rotation of the output shaft. Once the waves move the floater upwards, this compresses the vibrating system which absorbs some of the energy and then the vibrating system helps the floater return to its original position by releasing the stored energy. The vibrating system also serves as a control method for limiting rack movement, so the impact of the waves is not detrimental to the system. This article aims to approximate the optimized power input to the system and investigate whether the implementation of a novel vibrating system improves the system power input. Allowing the WEC's natural frequency to reach the wave's natural frequency is important as it allows for maximum power absorption. The use of vibration systems to tune the WEC's natural frequency close to the waves' is novel and serves as the main factor in choosing this research. The WEC was modeled as 2 spring mass damper systems. Then the characteristic equations of the systems were extracted from the equations of motion and solved analytically to obtain the responses. One-factor-at-a-time (OFAT) method together with two different algorithms (Genetic and Multi-Start algorithms) from MATLAB code were used to optimize the response. The optimized power input to the system was then approximated. For system one, the maximum amplitude of the response was seen at a system mass of 500 kg and stiffness in the range of $100 < k < 240$ N/m. The same was achieved for system two at a system mass of 500 kg and stiffness in the range of $100 < k < 138$. The effect of the stiffness and mass on the response and input power has also been discussed.

Keywords: Optimization; Wave Energy Converter; Auxiliary Vibrating System; Rack and Pinion PTO



@ The author(s). Published by CBIORE. This is an open access article under the CC BY-SA license (<http://creativecommons.org/licenses/by-sa/4.0/>).

Received: 23rd Oct 2022; Revised: 26th Dec 2022; Accepted: 8th Jan 2023; Available online: 18th Jan 2023

1. Introduction

Yoshio Masuda, a Japanese Naval Commander, is the father of modern wave power technology. Yoshio invented a navigation buoy that incorporated an air turbine that was powered by wave energy. Masuda, 1976 also went on to promote the construction of a barge known as Kaimei that housed several Oscillating Water Columns (OWCs) with different air-driven turbines (Falcão, 2010). This didn't garner great success as wave power generation was still in its nascent days. The 1970s oil crisis served as the stepping stone for academic research due to the increased prices of fossil fuels together with the restriction of oil supplies (Polinder & Scuotto, 2005). The arrival of the 1980s led to the reduction of oil prices which slowed down wave energy research due to the lack of funds (Ahamed et al., 2020). The European Commission in the 1990s paved the way for wave energy by funding research and development in the wave energy sector. Then after a couple of decades, interest in wave energy spiked again, this time driven by the pollution from fossil fuels, the rise in energy demands, and alarms of climate change (Ahamed et al., 2020). The oceans and seas contain colossal amounts of energy that are distributed throughout the world's shorelines. Estimates suggest that the

annual practical world wave energy resource is between 2000 TWh and 4000 TWh. (Brooke, 2003). Some recent estimates of the annual global theoretical wave energy potential hitting the coasts are between 8500 to 18500 TWh (Gunn & Stock-Williams, 2012). Solar energy is available only 30% of the time whereas wave energy is available 90% of the time. Additionally, power flow in ocean waves is up to five times more when compared to wind energy thereby making it more favorable than wind energy (Falnes, 2007). Wave power has the highest power density out of all renewable energies and its density, intermittency, and predictability give it significant advantages to power generation (Bedard & Hagerman, 2005). Less physical area is required by the wave energy converters to capture the same quantity of energy in contrast with other forms of renewable energy due to wave energy having more predictability than solar power and more continuity than wind power (Zullah et al., 2010).

The incorporation of renewable energy sources in the energy mix is vital for the development of sustainability. Czech and Bauer (2012) have described and evaluated a few important WECs (Czech & Bauer, 2012). Over the years, numerous patents have been filed for WECs, each claiming to be unique. The wave energy systems can be classified by using several methods that

* Corresponding author
Email: farid.mn83@gmail.com (F.M. Nasrekani)

depend on working principles (the mode of energy capture), location (Shoreline, Nearshore, Offshore), and the size of the WEC (Falcão, 2010). WECs can also be classified based on the ratio of the magnitude of the wavelength over the interacting part of the WEC (Aderinto & Li, 2018). They are attenuators, OWCs, overtopping terminators, and point absorbers. Attenuators are multi-segmented structures that lie parallel to the predominant wave direction and 'ride' the waves (Drew *et al.*, 2009) such as Pelamis Wave Power (EMEC, 2014). Henderson (2006) presented the development including the simulation and lab tests of the hydraulic PTO employed in the Pelamis WEC (Henderson, 2006).

OWCs consist of chambers with an opening to the sea that is below the waterline. Oncoming waves force the water into the chamber and apply pressure on the air present in the chamber which then escapes via a turbine. Air is drawn in through the turbine while the water retreats. Often, a low-pressure wells turbine is used in this application that rotates in the same direction regardless of the flow direction thereby eliminating the need for rectifying the airflow (Boyle, 2004). Overtopping terminators capture the incoming waves in a reservoir that is above sea level, and the water is released via turbines (Drew *et al.*, 2009). A popular illustration of overtopping terminators is the Wave Dragon (Wave Dragon, 2011). A prototype of Wave dragon 57 x 27 m² wide and 237 tonnes heavy was tested in Nissum Bredning, Denmark (Kofoed *et al.*, 2006). Point absorbers are devices whose dimensions are relatively small when compared to the incident wavelength. These are floating structures that 'bob' up and down on the water's surface. Wave direction does not matter, as these devices are small and generally installed in large arrays for instance Ocean Power Technology's 'Powerbuoy' (OPT, 2008). Some other point absorber devices are Aquabuoy, Wavebob, and Uppsala point absorber WEC (Faizal *et al.*, 2014). The Aquabuoy incorporates a floater that helps to keep the system afloat. Connected below the floater is a large cylinder called the accelerator tube which houses a piston that connects to the top and bottom sections of the buoy via a hose pump. The stretching and compression of the hose pump due to the relative motion of the buoy and the piston drives the water through a Pelton turbine (Wacher & Neilsen, 2010). The power matrix of three commercial WECs viz. Wave Dragon, Pelamis, and AquaBuoy were used to estimate the best scale factors that lead to the best Capacity Factor (CF) in the Leeward Islands. Wave Dragon was the most indicated device (CF=71% scaled by 0.3), followed by AquaBuoy (CF=57% at a scale of 0.4) and then Pelamis (CF=26% scaled by 0.5). The Cost to Benefit ratio (C/B) of the three devices was also found and in its natural state, AquaBuoy was found to be the most efficient device (Monteiro *et al.*, 2019). The Wavebob device uses a damping system that controls the two oscillating bodies. Sea water mass acts as a significant portion of inertial mass that is used by the semi-submerged body to tune the device to the average wave frequencies. The Wavebob contains an outer ring and an inner float. The outer ring provides a path for the inner float to slowly undergo heave motion. Electricity is generated through a high-pressure oil system by capturing the energy of the heave motion (Weber *et al.*, 2009). The Uppsala WEC makes use of a direct-driven permanent magnet linear generator which is positioned on the seabed. The moving part of the generator is connected to the buoy via a line and a piston. There are springs attached below the translator of the generator that stores energy while also acting as a restoring force during wave-throughs (Rahm *et al.*, 2010). Recently, there has been an increase in the research of point absorber WECs that incorporate rack and pinion type PTO. Liang *et al.* (2017) proposed a 1.2m single buoy WEC with

an MMR-based PTO system. This system integrates one-way bearings into a rack and pinion system, and this allows the conversion of bidirectional wave motion into a unidirectional movement of the generator. Simulations in regular waves show that MMR-based PTOs can produce more power in comparison to linear damping PTO (Liang *et al.*, 2017). Youssef *et al.* (2016) constructed a nearshore heaving-buoy WEC which contained a float-rack-pinion system that converts the vertical heaving motion of the waves into rotating motion. The system was connected to an alternator and shallow water (1-5m water depth) testing successfully light up a 3 W lamp. In order to utilize both the upward and the downward motion of the waves, two freewheel gears were mounted on a shaft that was directly connected to the alternator (Youssef *et al.*, 2016). Chandrasekaran & Sinhmar (2012) designed and modeled a Mechanical Wave Energy Converter and conducted experimental investigations to test its capability to generate power. The system included a floating buoy that moves upwards with the waves and rotates one pinion gear clockwise and rotates the other pinion gear anticlockwise when the floater is moving downwards. The freewheel sprockets rotate the generator shaft unidirectionally. The overall efficiency of the MWEC was 18.7% (Chandrasekaran & Harender, 2012). Hadano *et al.* (2016) tested a system consisting of a float, a shaft that connected to another shaft together with a rack and pinion mechanism that was connected to a rotary generator. The system was in an array of water chambers and set along the direction of the incident wave propagation. The system could be set up along jetties or long floating bodies to provide easier installation and maintenance access (Hadano *et al.*, 2017). Tri *et al.* (2018) presented an experimental study of a PTO system using a WEC that converted bidirectional wave motion into unidirectional motion, a flywheel, and an electro-hydraulic actuator (Tri *et al.*, 2018). Dang *et al.* (2019) proposed a new mechanism to achieve resonant behavior of point absorber WEC system with a rack and pinion type PTO. The resonant behavior was achieved through the design of hydraulic springs that help lower the effective stiffness of the float. The natural frequency of the device can be tuned close to the natural frequency of the wave with the new design implementation. An increase in power capture bandwidth and performance was seen when the buoy is in near resonance with the wave. The original WEC system used a rack and pinion type PTO coupled with a bidirectional gearbox to convert the heave motion of the wave into a unidirectional motion (Dang *et al.*, 2019). Leger Monteiro and Sarmiento (2019) analyzed the possibility of energy harvesting from ocean waves. This analysis was based on a period of 31 years of data (Monteiro *et al.*, 2019). Aminuddin *et al.* (2020) presented a numerical analysis for a wave energy power generation-pendulum system based on the Euler-Lagrange and Runge-Kutta formulations (Aminuddin *et al.*, 2020). Amin *et al.* (2021) designed and simulated a WEC consisting of a buoy and an MMR-based rack and pinion system in MATLAB/Simulink. They discussed the effective control method of using a rack and pinion type PTO and analyzed the performance of the whole system. The applied ratcheting method converted the up and down motion of the buoy into unidirectional motion. The unidirectional motion through a gearbox then drove a generator to produce electricity. The novel control mechanism did not require the prediction of the wave excitation force (Amin *et al.*, 2021). Kim and Cho (2021) studied the wave power extracted from multiple WECs deployed in a Y-shaped water channel (Kim & Cho, 2021). Jiang *et al.* (2021) presented a design and experimental study of a PTO system for Salter's Duck WEC. Salter's Duck WEC is capable to convert wave energy into mechanical energy with high

efficiency of about 90% (Jiang *et al.*, 2021). Do *et al.* (2022) presented a new control strategy for hydraulic PTO to increase efficiency by employing a hydraulic motor and a generator (Do *et al.*, 2022). Jahangir and Ghanbari Motlagh (2022) investigated the applications of a WEC which was called CETO to generate power on the Iranian coasts and analyzed the effect of grid extension cost and load change (Jahangir & Ghanbari Motlagh, 2022). Setyandito *et al.* (2022) studied the velocity magnitude of WEC systems by analyzing the relation between wave run-up, wave steepness, and relative velocity (Setyandito *et al.*, 2022).

Out of the various rack and pinion type WECs developed and tested, almost all depend on the wave motion and the weight force of the floater to help the buoy go back to the starting position. If the floater does not manage to go back to its starting position before the incoming waves arrive, it is jerked upwards again, and this sudden burst of energy is detrimental to the WEC. It is also important to note that effective controls should be built into the system so that the WECs are able to handle the highly energetic sea states occurring during cyclones. One such way to build the said control is by employing a vibrating system attached to the aquatake-off (PTO) of the WEC. With the proposed vibrating system in place, once the waves force the floater upwards, the vibrating system will absorb some of the energy and limit the range of the rack to safe levels and then release this energy to help the floater return to its starting point providing a means of generating continuous power. Continuous power generation is superior to intermittent power generation as discussed by (Hadano *et al.*, 2017). The transfer function in a vibrating system with a low-frequency ratio can be controlled by the stiffness and if the frequency of excitation increases, it can be controlled by damping and it depends on the frequency of the ocean waves and the system characteristics. It is noted that the response of this system will be directly converted to the output of the gearbox and by controlling the response, the output can be modified. This study aims to approximate the optimized power input to the system and investigate whether the implementation of a novel vibrating system would improve the system power input. The effect of the system mass and stiffness on the response and power input of the system will also be studied. Modeling the rack and pinion type WEC as a spring mass damper system, this study will obtain the optimized values of mass and spring stiffness that will maximize the response (buoy displacement) and the input power of the WEC. Initially, the optimization will be done via the trial-and-error method also known as the OFAT method. This is done to understand the effect of changing one parameter such as mass and spring stiffness on the response and eventually

obtaining an approximation of the input power. After the initial bases are covered, the same response will be optimized via MATLAB employing two different algorithms i.e., Genetic and Multi-Start algorithms. The proposed design and optimized system consider nine combinations of different cases of wave characteristics (e.g., minimum period and minimum height of the wave).

2. Proposed Model

This study focuses on point absorber type WEC with a rack and pinion type PTO. The overall system model contains a double rack, two compound pinion gears, a connecting rod, and a floater as shown in Fig. 1. The floater is semi-submerged into the water. The ocean waves apply excitation force to the floater thereby causing it to move up and down. The force from the waves creates torque to drive the compound pinions that are geared to the rack. The ratcheting mechanism (one-way bearings) installed in the pinion gears ensures that only one pinion gear is active while the rack is going up and vice versa.

There is also a spring-damper system attached to the top of the rack which will act as the vibrating system and help push the floater down to its original position. For this purpose, two models have been considered in this study as shown in Fig. 2, in which A and ω are the amplitude and frequency of the wave, respectively. The system damping is kept constant at 10 Ns/m. By employing the theory of vibrations for a single-degree freedom system, the equation of motion for both systems can be obtained as the following:

$$\text{System 1: } m \frac{d^2x(t)}{dt^2} + c \frac{dx(t)}{dt} + kx(t) = c \frac{dy(t)}{dt} + ky(t) \quad (1a)$$

$$\text{System 2: } m \frac{d^2x(t)}{dt^2} + c \frac{dx(t)}{dt} + kx(t) = A' \sin \omega t \quad (1b)$$

where m is the total mass of the rack and the additional mass to optimize the response, k is the stiffness of the auxiliary vibrating system, and c is the damping coefficient of the system. y is the wave equation, and it is obtained based on the wave height and period under different conditions of wave motion, and x is the displacement of the system from the equilibrium. In Eq. (1b), A' is the amplitude of the force applied to the system which is proportional to m , ω , A and the dimension of the floater.

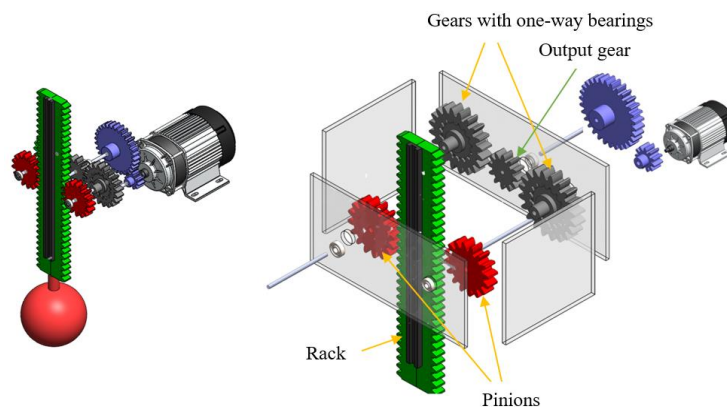


Fig. 1. Proposed gearbox and its components.

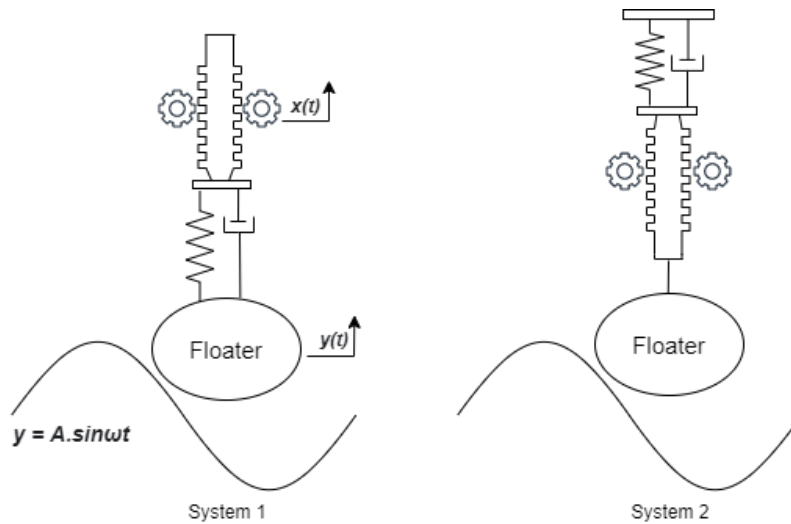


Fig. 2 Proposed auxiliary vibrating system attached to rack and pinion

Table 1
Wave Characteristics used in this Study

	Minimum	Average	Maximum
Wave Height- <i>Y</i> (m)	0.5	2.25	4
Wave Period- <i>T</i> (s)	10	12	14

The analysis was done for three different wave heights and periods. The minimum and maximum wave heights were taken from a site (Ram *et al.*, 2014), then the average wave height was calculated from the maximum and minimum wave heights. The same was done for the wave periods. The wave characteristics used for this study are reported in Table 1. There are 9 total cases for each system.

The first step was to obtain the response of the system when the system is under the effect of base excitation. The equation of motions of both systems (Eqs. (1a,1b)) was used to find the characteristic equations. Then the characteristic equation was solved parametrically to find the homogenous (transient) and particular (steady-state) responses. Since the homogeneous form of equations is the same, the homogeneous response for both systems will be the same. The characteristic equation for both systems is as the following:

$$m\alpha^2 + c\alpha + k = 0 \tag{2}$$

where α is the eigenvalue of the system. By solving Eq. (2), two eigenvalues of the system will be obtained, and the homogenous solution is obtained as the following:

$$x_h(t) = C_1 e^{\left(\frac{-c + \sqrt{c^2 - 4km}}{2m}\right)t} + C_2 e^{\left(\frac{-c - \sqrt{c^2 - 4km}}{2m}\right)t} \tag{3}$$

where C_1 and C_2 are constant coefficients, and they are obtained by applying the initial conditions. The particular response for both systems has been considered as the following:

$$x_p(t) = C_3 \sin \omega t + C_4 \cos \omega t \tag{4}$$

where C_3 and C_4 are constant coefficients, and they are obtained by substituting into the nonhomogeneous form of equations.

These coefficients for each system are determined as the following:

$$\text{System 1: } C_3 = \frac{A(c^2\omega^2 - km\omega^2 + k^2)}{m^2\omega^4 + c^2\omega^2 - 2km\omega^2 + k^2}, \quad C_4 = \frac{-Acm\omega^3}{m^2\omega^4 + c^2\omega^2 - 2km\omega^2 + k^2} \tag{5a}$$

$$\text{System 2: } C_3 = \frac{A'(-m\omega^2 + k)}{m^2\omega^4 + c^2\omega^2 - 2km\omega^2 + k^2}, \quad C_4 = \frac{-A'c\omega}{m^2\omega^4 + c^2\omega^2 - 2km\omega^2 + k^2} \tag{5b}$$

The total response is the summation of homogeneous and nonhomogeneous solutions as follows:

$$x = x_h(t) + x_p(t) \tag{6}$$

where the particular solution ($x_p(t)$) for system 1 and 2 is determined from Eq. (5a) and (5b), respectively. The response was differentiated to obtain the velocity of the system and double differentiated to find the acceleration of the system. Applying Newton's second law and transmitted force in vibrating system, the applied force to the pinion gears and generated torque have been obtained. The input power to the system has been calculated as the following:

$$P_{in} = T \cdot \Omega \tag{7}$$

where T and Ω , are the applied torque and angular velocity of the pinion gears. Using the relationship between torque and force, we can calculate the input power to the WEC as a function of vibrating system parameters. For this purpose, the applied torque and angular velocity are determined as the following:

$$T = F \cdot r, \quad \Omega = \frac{1}{r} \frac{dx}{dt} \quad (8)$$

where F and r are the applied/transmitted force and radius of pinion gears. The transmitted force in both the vibrating systems can be approximated by $F=ma$, which a is the acceleration of the system. Finally, the input power as a function of the response is obtained as the following:

$$P_{in} = m \cdot \frac{d^2x}{dt^2} \cdot \frac{dx}{dt} \quad (9)$$

It is observed that to optimize the input power we need to optimize the response. Also, it should be considered that the input power depends on the total mass of the system and by increasing the mass, the power will be increased, while, in some cases by increasing the mass, the response amplitude might decrease. Therefore, it is necessary to optimize the system by considering all these parameters.

3. Optimization

In most of the engineering applications and industries, optimization has become an optimum tool to determine the most favorable response. Optimization process usually requires the evaluation of an objective function multiple times. Increased demand for accuracy and increased complexity of designs requires high running time for simulations, this is where optimization algorithms are employed in reducing the simulation time (Kolda *et al.*, 2003). An efficient optimization algorithm is tremendously important to reach complex linear and non-linear solutions (Hooke & Jeeves, 1961; Yang, 2013).

First by employing trial and error and considering one variable, OFAT approach has been used to obtain the optimum response. The response of the system is such as a sinusoidal diagram with amplitude X . The two parameters chosen to be optimized were the system mass and stiffness. The optimization of the system mass and stiffness would result in the maximum amplitude of the response. Since by maximizing the amplitude of the response, the velocity, acceleration, and consequently the input power will be maximized, the purpose of the optimization is to maximize the amplitude of the response. In addition to the OFAT approach, the MATLAB optimization toolbox has been employed to verify the solutions obtained with OFAT. Two Different algorithms are used to optimize the response.

Optimization based on the Genetic algorithm was done in MATLAB Live Editor using the Task > Optimize option. The optimize Live Editor Task in MATLAB enables users to interactively set up and run optimization solvers with ease. First, the problem type (Nonlinear), constraints (Lower and Upper bounds), and solver were set up. Then the objective function, initial point, and constraint values were set up. The objective functions were obtained from Eq. (6) with the values of T and Y (wave period and height) being changed as per the case. The constraints were the Lower and the Upper bounds in our case. The system mass was bounded between 10 and 500 kg whereas the system stiffness was bounded between 70 and 1000 N/m. The constraints used for both algorithms are the same. The initial point setup for both algorithms was the same where the system mass was 10 kg, and the system stiffness was 70 N/m. Occasionally some solver options such as 'Run time limits' and Mesh Size were changed to reach the optimum results. The Multi-Start algorithm was done in MATLAB scripts. This required manual setup of all the parameters and options, unlike the Live editor tasks. First, the Problem Structure was created using the 'createOptimProblem' function. The solver object was

then created which contains the different properties of the optimization such as Global Options. The final step was to run the solvers.

The Genetic algorithm adheres to the Darwinian theory of natural selection, also known as the "survival of the fittest". Stating that the fittest offspring gives either the principal solution or will ensure to the production of the fittest set of offspring. A Genetic algorithm is a successor of the traditional evolutionary algorithm. In simple terms it will select random solutions from the available data, to utilize it again to reproduce the next generation of data using biological operators such as reproduce, select, mutation, and crossover (Immanuel & Chakraborty, 2019). However, in some cases, Genetic algorithms show stagnation in local minima and other alternative algorithms such as pattern search optimization. It was observed in this study that genetic algorithms need a good starting point and strict bound (upper and lower) setup to avoid stagnation in local minima. Multiple ideas were suggested to avoid the local minimal stagnation, one of them was to re-start the search for a new solution once ample exploration was done on a certain region. This was further developed as the Multi-Start algorithm. The Multi-Start algorithm starts off by checking the validity of the input arguments. A set of random points is then generated within the specified bounds. Then the algorithm uses a local solver usually 'fmincon' to seek a local solution from a solution of the generated points. Once the solver completes all the points, a vector 'GlobalOptimSolutin' is created that contains the function value from best to lowest (MATLAB, 2010). The optimization has been utilized with respect to the stiffness of the system (k) and the system's total mass (m). All the nine possible conditions of wave characteristics based on the data in Table 1 have been considered for the optimization procedure.

4. Results and Discussion

To conduct a parametric study and trial error procedure for the OFAT approach, one mathematical code based on the analytical solution in MAPLE has been prepared. In this step, one of the variables (i.e., m or k) is considered as a constant value and the response amplitude for different cases has been obtained. Fig. 3 shows the effect of the stiffness and total mass on the response amplitude in system one for the case of average period and minimum amplitude of the wave. It is seen that by increasing the total mass, the amplitude is increasing for a specific range of stiffness. For instant, in the case $m=200$ kg, for the range of stiffness $0 < k < 100$ N/m, by increasing the stiffness, the amplitude increases and for $k > 100$ N/m, the amplitude drops as the stiffness increases. In the studied range of parameters, the maximum amplitude has been obtained for the case $m=510$ kg and $k=180$ N/m. The same behavior is observed for the variation of the total mass. The same results are obtained for other cases of the wave characteristics which are not reported here.

Fig. 4 shows the effect of the variations of the stiffness and total mass on the response amplitude in system two for the case of average period and minimum amplitude of the wave. The same results as system one can be concluded from system two. As a result, by increasing the stiffness and the total mass, the amplitude of the response increases. Of course, it should be considered that the increment in the response happens in a specific range of the other parameter. For example, for the case $m=180$, for $k > 100$, the amplitude drops significantly. Therefore, to find the maximum value of the amplitude, it is necessary to consider the effects of both mass and stiffness at the same time. The same results are extracted for other cases of the wave characteristics which are not reported here.

For each case of the wave characteristics, the graphs of the response amplitude have been plotted and by try and error the optimum values for the stiffness and the total mass of the system have been determined to achieve a maximum amplitude in the

response. For example, for the studied range, the maximum amplitude in system two occurs for the case, $m=600$ kg and $k=100$ N/m.

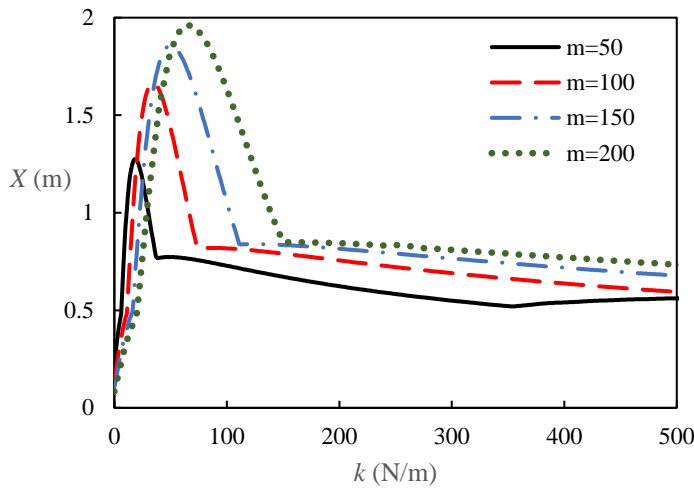


Fig. 3a Amplitude versus stiffness for different value of mass in system one (T_{avg} , Y_{min})

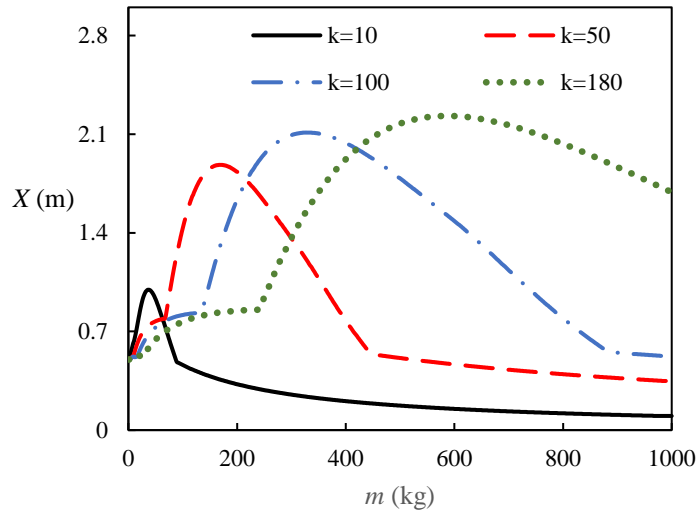


Fig. 3b Amplitude versus total mass for different value of stiffness in system one (T_{avg} , Y_{min})

Table 2
Optimum values of stiffness and total mass for system one

T	Y	Try & Error			Genetic Algorithm			Multi-Start Algorithm		
		X	k	m	X	k	m	X	k	m
Min	Min	2.19	230	500	2.23	242.3	500	2.23	242.3	500
Min	Avg	9.81	210	450	10	210.2	457.2	10	210.2	457.2
Min	Max	17.59	240	500	17.8	242.3	500	17.8	242.2	500
Avg	Min	2.17	160	500	2.21	159.6	500	2.21	159.5	500
Avg	Avg	9.87	160	500	9.93	159.6	500	9.93	159.5	500
Avg	Max	17.1	160	500	17.6	159.3	500	17.6	159.5	500
Max	Min	2.17	120	500	2.18	119.5	500	2.18	119.4	500
Max	Avg	9.80	120	500	9.80	119.5	500	9.80	119.4	500
Max	Max	17.4	120	500	17.4	119.5	500	17.4	119.4	500

The maximum system response and the optimum values of the stiffness (k) and total mass (m) obtained via the try and error method and two different algorithms are reported in Table 2 for system one. The trial-and-error method first varied mass in the response equation while the stiffness was kept constant and vice versa. The optimum value of mass was reached when further increasing the mass did not result in any significant increase of the response. The same was done for the stiffness. It is observed that the results of try and error are in good agreement with the optimization algorithms' results. Also, it is concluded that in system one configuration, $m=500$ is the optimum value for all the cases of wave characteristics. However, to obtain a general optimum value for the stiffness we need to consider a statistical analysis to obtain that in a specific period of time (e.g., one year) which cases are much more observed. Generally, stiffness in the range of $100 < k < 240$ causes an acceptable optimum response in all cases. It should be noted that the presented results are based on theoretical calculations and some of them are not practical and causes irrational dimensions in the system. However, the behavior of the system is the purpose of this study to investigate the effect of the vibrating system on the WEC unit and optimization of the vibrating system components.

Table 3 reports the response amplitude and optimum values of the stiffness, and mass obtained by try and error, Genetic, and Multi-Start algorithms. Like system one, it is observed that $m=500$ is an optimum value for the total mass in all cases. In system two, the general optimum value for the stiffness is in a smaller range and it should be in the range of $100 < k < 138$. Therefore, to have a maximum amplitude in the response and consequently a maximum input power in the system's two configurations, we need to adjust the total mass to 500 and the stiffness must be in the range of 100 and 138.

To investigate the effect of the vibrating system on the WEC response, Fig. 5 shows the steady-state response of system one in case T_{min} and Y_{min} for the WEC with and without an auxiliary vibrating system. It is seen that by employing the auxiliary vibrating system, the amplitude of the response has increased significantly. The same results are obtained for system two and other cases of wave characteristics. Moreover, it should be noted that by employing the vibrating system, the frequency of the response has increased as well. By employing the vibrating system, the amplitude of the response has increased six times and consequently, the velocity which is the derivative of the response with respect to time, will increase significantly. By increasing the velocity, the harvested energy also increases.

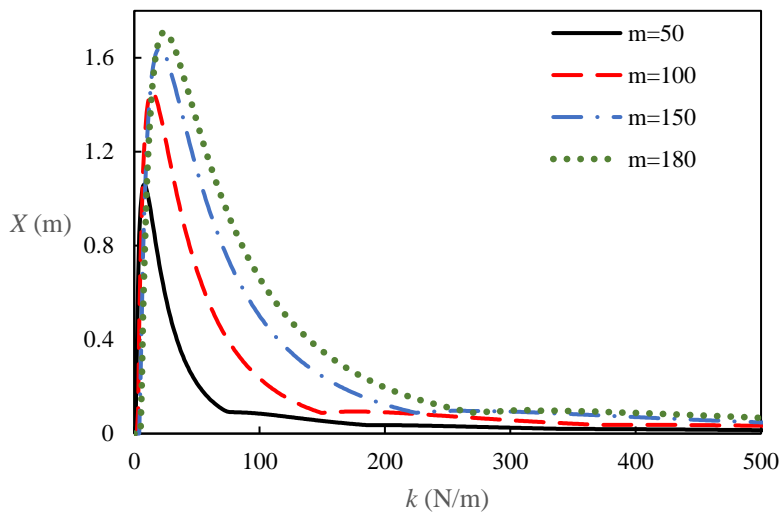


Fig. 4a Amplitude versus stiffness for different value of mass in system two (T_{avg} , Y_{min})

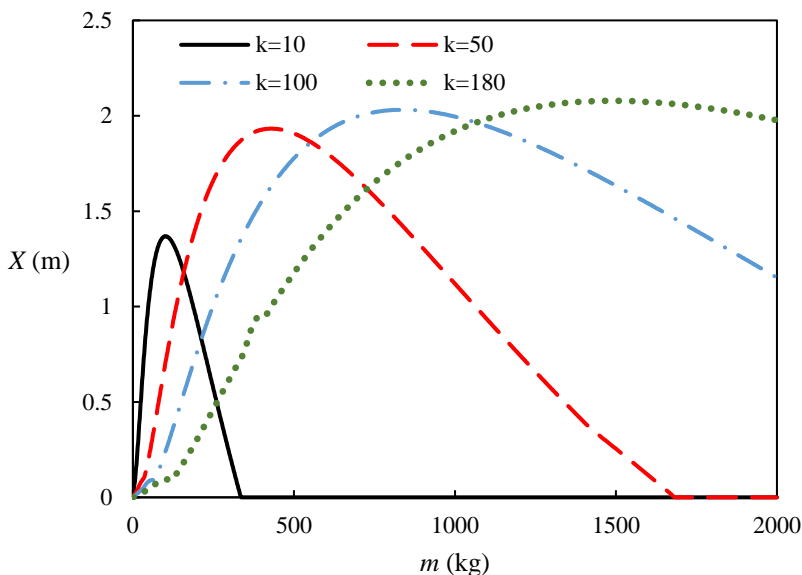


Fig. 4b Amplitude versus total mass for different value of stiffness in system two (T_{avg} , Y_{min})

Table 3
Optimum values of stiffness and total mass for system two

T	Y	Try & Error			Genetic Algorithm			Multi-Start Algorithm		
		X	k	m	X	k	m	X	k	m
Min	Min	2.46	135	500	2.49	137.9	500	2.49	138	500
Min	Avg	11.0	135	500	11.2	137.9	500	11.2	138	500
Min	Max	19.4	140	500	19.9	138.1	499	19.9	138	500
Avg	Min	2.28	95	500	2.45	100	500	2.45	96.1	500
Avg	Avg	10.8	95	500	11.0	100	500	11.0	96.1	500
Avg	Max	19.4	95	500	19.6	96.15	500	19.6	96.1	500
Max	Min	1.92	100	500	1.94	104.8	500	1.94	105	500
Max	Avg	8.72	100	500	8.74	104.8	500	8.74	105	500
Max	Max	15.4	100	500	15.5	104.8	500	15.5	105	500

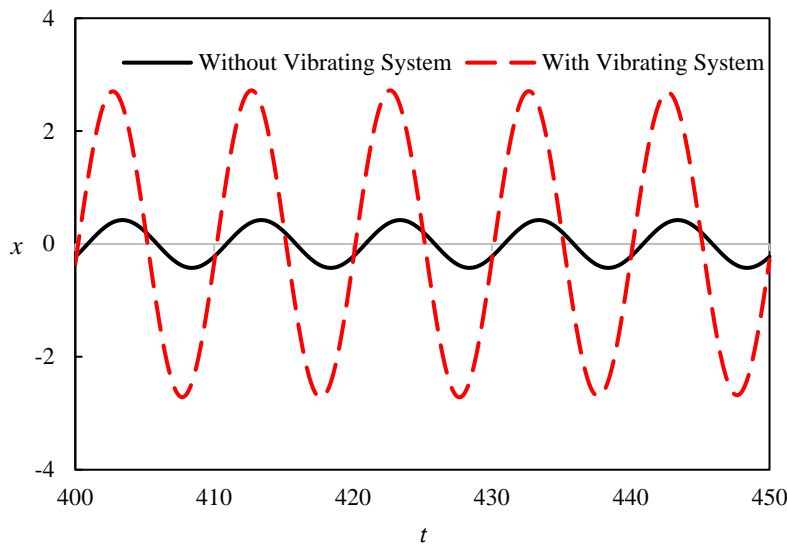


Fig. 5 Steady-state response of WEC with and without auxiliary vibrating system (system one)

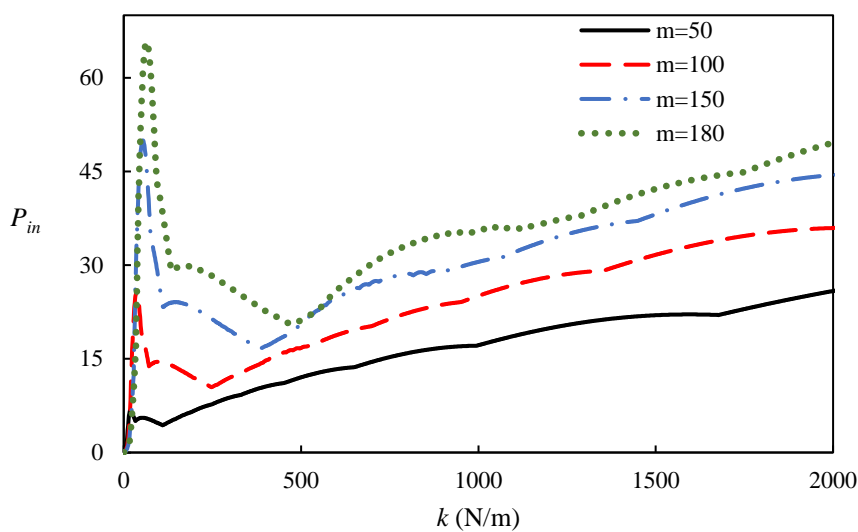


Fig. 6 Input power versus stiffness for system one (T_{avg} , Y_{min})

Table 4
Power Input Comparison between OFAT and Algorithms

System	T	Y	Try & Error			Genetic Algorithm		
			P_{in} (W)	k (N/m)	m (kg)	P_{in} (W)	k (N/m)	m (kg)
1	Min	Min	423	230	500	428	242	500
	Min	Avg	7904	210	450	7912	210.2	457.253
	Min	Max	28198	240	500	28205	242.4	500
	Avg	Min	245	160	500	243	159.5	500
	Avg	Avg	4921	160	500	4952	159.5	500
	Avg	Max	15505	160	500	15562	159.5	500
	Max	Min	84	120	500	84	119.5	500
	Max	Avg	1698	120	500	1686	119.5	500
	Max	Max	5390	120	500	5391	119.5	500
2	Min	Min	350	135	500	352	137.9	500
	Min	Avg	7045	135	500	7050	137.9	500
	Min	Max	22275	140	500	22282	138.1	500
	Avg	Min	119	95	500	123	100	500
	Avg	Avg	2514	95	500	2520	100	500
	Avg	Max	7942	95	500	7965	100	500
	Max	Min	65	100	500	67	104.8	500
	Max	Avg	1368	100	500	1370	104.8	500
	Max	Max	4339	100	500	4349	104.8	500

The maximum system input power obtained from the try and error method and the said algorithms are shown in Table 4. The max power input to the system and the dependent parameters are obtained for all the cases by try and error method as well as the Genetic algorithm. As it was expected, the maximum power was achieved with the same value of optimum parameters reported in the previous section for the response, and the m and k for the responses obtained in Table 2 and Table 3 resulted in the optimum power inputs. It is also seen that an increase in wave period reduces the maximum power input for the same wave heights and by increasing the wave height, the power increases for the same value of wave period.

The input power is plotted versus mass and stiffness for system one and system two, which results in the same conclusions as the response and are not reported here. However, in some cases by increasing the mass, the input power increases without any bond. Fig. 6 shows the input power versus the stiffness for different values of mass in system one. As it is seen, the input power has increased as the total mass and stiffness increase, and the input power has a different behavior from the response for $k > 500$. In fact, the reason is the effect of m in Eq. (8) on the input power. However, theoretically, the optimum value of the input power has been achieved in the optimum parameters as reported in Table 3. It was shown by Setyandito *et al.* (2022) that by increasing the velocity of wave, the harvested energy has been increased. The same results can be concluded from the presented method. By optimizing the mass and stiffness, and achieving the maximum value for the displacement, the maximum value for velocity will also be reached (Eq. (6) and its derivatives). Consequently, the harvested energy, and power will be maximized as it is seen in Table 4 and Fig. 6. By adjusting the mass and stiffness

parameters, the natural frequency of the presented system can reach the frequency of waves and a semi-resonance phenomenon will happen which increases the harvested power (Kim & Cho, 2021). This conclusion can be observed in the presented results.

5. Conclusion

This paper presents a novel vibrating system that can be implemented to improve the power input to a WEC with a rack and pinion type PTO in regular waves. The response of the system was extracted and the OFAT method was used to estimate the optimum system parameters to maximize the response. The response of the system was then optimized in MATLAB using two different algorithms namely: Genetic and Multi-Start. The OFAT and MATLAB optimization results were in good agreement. The optimized system parameters were then used to approximate the power input to the device. The vibrating system doubles as a control method to smoothen the impact of the waves on the device as well as to increase the input power absorbed by the system. It should be noted that the theoretical extracted results are based on the range of studies for the parameters. It was seen that as the total mass increases, the amplitude of the response and input power increase for a specific range of stiffness and as the stiffness increases, the amplitude of the response and input power increase for a specific range of the total mass. The effect of the mass on the input power is more significant than its effect on the response amplitude. An increase in wave period causes a drop in the maximum input power and by increasing the wave height, the power increases. For system one, $m=500$ and stiffness in the range of $100 < k < 240$, results in the maximum amplitude in the

response. For system two, $m=500$ and stiffness in the range of $100 < k < 138$, causes the maximum amplitude in the response.

Conflict of Interest Statement

On behalf of all authors, the corresponding author states that there is no conflict of interest.

References

- Aderinto, T., & Li, H. (2018). Ocean Wave Energy Converters: Status and Challenges. *Energies*, 11(5), 1250–1276. <https://doi.org/10.3390/en11051250>
- Ahamed, R., McKee, K., & Howard, I. (2020). Advancements of wave energy converters based on power take off (PTO) systems: A review. *Ocean Engineering*, 204, 107248–107273. <https://doi.org/10.1016/j.oceaneng.2020.107248>
- Amin, M. S., Bora Karayaka, H., Yanik, P., & Sang, Y. (2021). Suboptimal Control of a Rack and Pinion Based Wave Energy Converter Power Take-off System. *SoutheastCon 2021*, 1–7. <https://doi.org/10.1109/SoutheastCon45413.2021.9401831>
- Aminuddin, J., Effendi, M., Nurhayati, N., Widiyanti, A., Razi, P., Wihantoro, W., Aziz, A. N., Abdullatif, R. F., Sunardi, S., Bilalodin, B., & Arifin, A. (2020). Numerical Analysis of Energy Converter for Wave Energy Power Generation-Pendulum System. *International Journal of Renewable Energy Development*, 9(2), 255–261. <https://doi.org/10.14710/ijred.9.2.255-261>
- Bedard, R. and Hagerman, G. Electric Power Research Institute Electricity Innovation Institute Global Energy Partners LLC Virginia Polytechnic Institute and State University Mirko Previsic Consulting National Renewable Energy Laboratory (U.S.) & Energetics Inc. (2005). Offshore wave power feasibility demonstration project: project definition study final summary report. EPRI.
- Boyle, G. (2004). *Renewable Energy: Power for a Sustainable Future* (2nd ed.). Oxford University Press.
- Brooke, J. (2003). *Wave Energy Conversion* (R. Bhattacharyya & M. McCormick, Eds.; 1st ed., Vol. 6). Elsevier Science.
- Chandrasekaran, S., & Harender. (2012). Power Generation Using Mechanical Wave Energy Converter. *The International Journal of Ocean and Climate Systems*, 3(1), 57–70. <https://doi.org/10.1260/1759-3131.3.1.57>
- Czech, B., & Bauer, P. (2012). Wave Energy Converter Concepts: Design Challenges and Classification. *IEEE Industrial Electronics Magazine*, 6(2), 4–16. <https://doi.org/10.1109/MIE.2012.2193290>
- Dang, T. D., Phan, C. B., & Ahn, K. K. (2019). Design and Investigation of a Novel Point Absorber on Performance Optimization Mechanism for Wave Energy Converter in Heave Mode. *International Journal of Precision Engineering and Manufacturing-Green Technology*, 6(3), 477–488. <https://doi.org/10.1007/s40684-019-00065-w>
- Do, T. C., Dang, T. D., & Ahn, K. K. (2022). Efficiency Improvement of a Hydraulic Power Take-off of Wave Energy Converter Using Variable Displacement Motor. *International Journal of Precision Engineering and Manufacturing-Green Technology*, 9(4), 1087–1099. <https://doi.org/10.1007/s40684-021-00371-2>
- Drew, B., Plummer, A. R., & Sahinkaya, M. N. (2009). A review of wave energy converter technology. *Proceedings of the Institution of Mechanical Engineers, Part A: Journal of Power and Energy*, 223(8), 887–902. <https://doi.org/10.1243/09576509JPE782>
- EMEC. (2014). *PELAMIS WAVE POWER*. The European Marine Energy Centre LTD. <https://www.emec.org.uk/about-us/wave-clients/pelamis-wave-power/>
- Faizal, M., Ahmed, M. R., & Lee, Y.-H. (2014). A Design Outline for Floating Point Absorber Wave Energy Converters. *Advances in Mechanical Engineering*, 6, 846097. <https://doi.org/10.1155/2014/846097>
- Falcão, A. F. de O. (2010). Wave energy utilization: A review of the technologies. *Renewable and Sustainable Energy Reviews*, 14(3), 899–918. <https://doi.org/10.1016/j.rser.2009.11.003>
- Falnes, J. (2007). A review of wave-energy extraction. *Marine Structures*, 20(4), 185–201. <https://doi.org/10.1016/j.marstruc.2007.09.001>
- Gunn, K., & Stock-Williams, C. (2012). Quantifying the global wave power resource. *Renewable Energy*, 44, 296–304. <https://doi.org/10.1016/j.renene.2012.01.101>
- Hadano, K., Lee, K. Y., & Moon, B. Y. (2017). Wave energy conversion utilizing vertical motion of water in the array of water chambers aligned in the direction of wave propagation. *International Journal of Naval Architecture and Ocean Engineering*, 9(3), 239–245. <https://doi.org/10.1016/j.ijnaoe.2016.06.002>
- Henderson, R. (2006). Design, simulation, and testing of a novel hydraulic power take-off system for the Pelamis wave energy converter. *Renewable Energy*, 31(2), 271–283. <https://doi.org/10.1016/j.renene.2005.08.021>
- Hooke, R., & Jeeves, T. A. (1961). "Direct Search" Solution of Numerical and Statistical Problems. *Journal of the ACM*, 8(2), 212–229. <https://doi.org/10.1145/321062.321069>
- Immanuel, S. D., & Chakraborty, U. Kr. (2019). Genetic Algorithm: An Approach on Optimization. *2019 International Conference on Communication and Electronics Systems (ICCES)*, 701–708. <https://doi.org/10.1109/ICCES45898.2019.9002372>
- Jahangir, M. H., & Ghanbari Motlagh, S. (2022). Feasibility study of CETO wave energy converter in Iranian coastal areas to meet electrical demands (a case study). *Energy for Sustainable Development*, 70, 272–289. <https://doi.org/10.1016/j.esd.2022.07.017>
- Jiang, Y., Peng, Y., Sun, Y., Zong, Z., & Sun, L. (2021). Design and Testing of a Mechanical Power Take-off System for Rolling-type Wave Energy Converter. *International Journal of Precision Engineering and Manufacturing-Green Technology*, 8(5), 1487–1499. <https://doi.org/10.1007/s40684-020-00253-z>
- Kim, J., & Cho, I.-H. (2021). Wave power extraction by multiple wave energy converters arrayed in a water channel resonator. *International Journal of Naval Architecture and Ocean Engineering*, 13, 178–186. <https://doi.org/10.1016/j.ijnaoe.2021.02.004>
- Kofoed, J. P., Frigaard, P., Friis-Madsen, E., & Sørensen, H. Chr. (2006). Prototype testing of the wave energy converter wave dragon. *Renewable Energy*, 31(2), 181–189. <https://doi.org/10.1016/j.renene.2005.09.005>
- Kolda, T. G., Lewis, R. M., & Torczon, V. (2003). Optimization by Direct Search: New Perspectives on Some Classical and Modern Methods. *SIAM Review*, 45(3), 385–482. <https://doi.org/10.1137/S003614450242889>
- Liang, C., Ai, J., & Zuo, L. (2017). Design, fabrication, simulation and testing of an ocean wave energy converter with mechanical motion rectifier. *Ocean Engineering*, 136, 190–200. <https://doi.org/10.1016/j.oceaneng.2017.03.024>
- MATLAB. (2010). *How GlobalSearch and MultiStart Work*. MathWorks. <https://au.mathworks.com/help/gads/how-globalsearch-and-multistart-work.html>
- Monteiro, L., Sarmento, A., & Madaleno, W. (2019). Analysing the Possibility of Extracting Energy from Ocean Waves in Cabo-Verde to Produce Clean Electricity - Case-Study: the Leeward Islands. *International Journal of Renewable Energy Development*, 8(1), 103. <https://doi.org/10.14710/ijred.8.1.103-112>
- OPT. (2008). *PB3 PowerBuoy*. Ocean Power Technology. <https://oceanpowertechologies.com/platform/opt-pb3-powerbuoy/>
- Polinder, H., & Scuotto, M. (2005). Wave energy converters and their impact on power systems. *2005 International Conference on Future Power Systems*, 1–9. <https://doi.org/10.1109/FPS.2005.204210>
- Rahm, M., Boström, C., Svensson, O., Grabbe, M., Bülow, F., & Leijon, M. (2010). Offshore underwater substation for wave energy converter arrays. *IET Renewable Power Generation*, 4(6), 602–612. <https://doi.org/10.1049/iet-rpg.2009.0180>
- Ram, K., Narayan, S., Ahmed, M. R., Nakavulevu, P., & Lee, Y. H. (2014). In situ near-shore wave resource assessment in the Fiji Islands. *Energy for Sustainable Development*, 23, 170–178. <https://doi.org/10.1016/j.esd.2014.09.002>
- Setyandito, O., Nizam, N., Pierre, A. J., Putra, G. D., Wijayanti, Y., & Anda, M. (2022). Numerical Analysis of Velocity Magnitude on

- Wave Energy Converter System in Perforated Breakwater. *International Journal of Renewable Energy Development*, 11(1), 27–33. <https://doi.org/10.14710/ijred.2022.38535>
- Tri, N. M., Binh, P. C., & Ahn, K. K. (2018). Power take-off system based on continuously variable transmission configuration for wave energy converter. *International Journal of Precision Engineering and Manufacturing-Green Technology*, 5(1), 89–101. <https://doi.org/10.1007/s40684-018-0010-0>
- Wacher, A., & Neilsen, K. (2010). Mathematical and Numerical Modeling of the AquaBuOY Wave Energy Converter. *Industry Case Studies Journal*, 2, 16–33. <http://www.fields.utoronto.ca/journalarchive/mics/13-20.pdf>
- Wave Dragon. (2011). *The Wave Dragon Technology*. Wave Dragon ApS. <http://wavedragon.net/>
- Weber, J., Mouwen, F., Parish, A., & Robertson, D. (2009). Wavebob – Research & Development Network and Tools in the Context of Systems Engineering. *8th European Wave and Tidal Energy Conference (EWTEC 2009)*, 416–420. [http://www.homepages.ed.ac.uk/shs/Wave%20Energy/EWT%20EC%202009/EWTEC%202009%20\(D\)/papers/207.pdf](http://www.homepages.ed.ac.uk/shs/Wave%20Energy/EWT%20EC%202009/EWTEC%202009%20(D)/papers/207.pdf)
- Yang, X.-S. (2013). Optimization and Metaheuristic Algorithms in Engineering. In *Metaheuristics in Water, Geotechnical and Transport Engineering* (pp. 1–23). Elsevier. <https://doi.org/10.1016/B978-0-12-398296-4.00001-5>
- Youssef, J., Matar, J., Rahme, P., & Bou-Mosleh, C. (2016). A Nearshore Heaving-Buoy Sea Wave Energy Converter for Power Production. *Procedia Engineering*, 145, 136–143. <https://doi.org/10.1016/j.proeng.2016.04.032>
- Zullah, M. A., Prasad, D., Ahmed, M. R., & Lee, Y.-H. (2010). Performance analysis of a wave energy converter using numerical simulation technique. *Science in China Series E: Technological Sciences*, 53(1), 13–18. <https://doi.org/10.1007/s11431-010-0026-3>



© 2023. The Author(s). This article is an open access article distributed under the terms and conditions of the Creative Commons Attribution-ShareAlike 4.0 (CC BY-SA) International License (<http://creativecommons.org/licenses/by-sa/4.0/>)